

Time-like Baryon Form Factors and Dispersion Relations

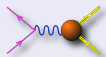
Simone Pacetti



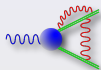
Electromagnetic Interactions with Nucleons and Nuclei



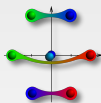
Milos Conference Center George Eliopoulos
Milos Island, September 28 - October 2, 2009



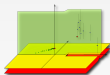
Threshold behavior in $e^+e^- \rightarrow p\bar{p}$



Other charged baryons cross sections



$e^+e^- \rightarrow \Lambda\bar{\Lambda}, \Sigma^0\bar{\Sigma}^0, \Lambda\bar{\Sigma}^0$ puzzle

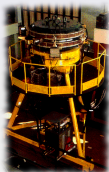


Space and time-like G_E^p/G_M^p via DR's

Bruno Touschek (1921, 1978) was an Austrian physicist, initiator of research on electron-positron colliders. He graduated from the University of Göttingen in 1946. He worked at the Max Planck Institute and at Glasgow. In 1952 he received the position of researcher at the National Laboratories of the Istituto Nazionale di Fisica Nucleare in Frascati.



Bruno Touschek (1921, 1978) was an Austrian physicist, initiator of research on electron-positron colliders. He graduated from the University of Göttingen in 1946. He worked at the Max Planck Institute and at Glasgow. In 1952 he received the position of researcher at the National Laboratories of the Istituto Nazionale di Fisica Nucleare in Frascati.



The first electron-positron collider was the "Anello di Accumulazione" (AdA), built by Bruno Touschek in Frascati (Rome) in 1960.

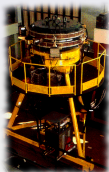


MAGNETIC DISCUSSION

Bruno Touschek



Bruno Touschek (1921, 1978) was an Austrian physicist, initiator of research on electron-positron colliders. He graduated from the University of Göttingen in 1946. He worked at the Max Planck Institute and at Glasgow. In 1952 he received the position of researcher at the National Laboratories of the Istituto Nazionale di Fisica Nucleare in Frascati.

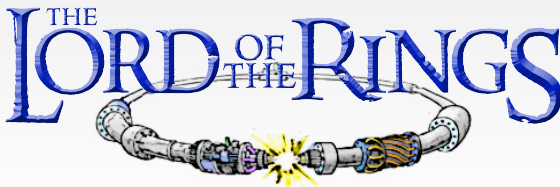


The first electron-positron collider was the "Anello di Accumulazione" (AdA), built by Bruno Touschek in Frascati (Rome) in 1960.



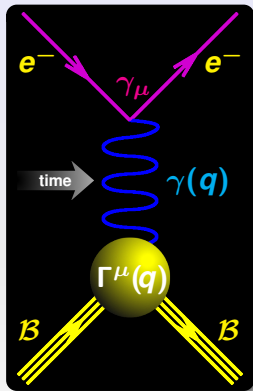
MAGNETIC DISCUSSION

Bruno Touschek



Baryon Form Factors definition

Space-like region ($q^2 < 0$)



- **Electromagnetic current** ($q = p' - p$)

$$J^\mu = e\bar{u}(p')\Gamma^\mu u(p) = e\bar{u}(p')\left[\gamma^\mu F_1(q^2) + \frac{i\sigma^{\mu\nu}q_\nu}{2M} F_2(q^2)\right]u(p)$$

- **Dirac and Pauli form factors F_1 and F_2 are real**

- **In the Breit frame**

$$\begin{cases} p = (E, -\vec{q}/2) \\ p' = (E, \vec{q}/2) \\ q = (0, \vec{q}) \end{cases} \quad \begin{cases} \rho_q = J^0 = e \left[F_1 + \frac{q^2}{4M^2} F_2 \right] \\ \vec{J}_q = e\bar{u}(p')\vec{\gamma}u(p) [F_1 + F_2] \end{cases}$$

$$\bullet 2M\bar{u}(p')\gamma^\mu u(p) = \bar{u}(p')[(p + p')^\mu + i\sigma^{\mu\nu}q_\nu]u(p)$$

$$\bullet \bar{u}(-\vec{p})u(\vec{p}) = E/M$$

$$\bullet u^\dagger(-\vec{p})u(\vec{p}) = 1$$

- **Sachs form factors**

$$G_E = F_1 + \frac{q^2}{4M^2} F_2$$

$$G_M = F_1 + F_2$$

- **Normalizations**

$$F_1(0) = Q_B$$

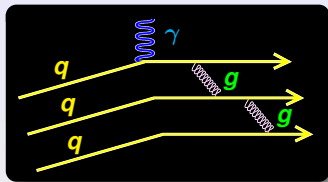
$$G_E(0) = Q_B$$

$$F_2(0) = \kappa_B$$

$$G_M(0) = \mu_B$$

pQCD asymptotic behavior

Space-like region



- **pQCD:** as $q^2 \rightarrow -\infty$, asymptotic behaviors of F_1 and F_2 must follow counting rules
- Quarks exchange gluons to distribute momentum

Dirac form factor F_1

- Non-spin flip
- Two gluon propagators
- $F_1(q^2) \underset{q^2 \rightarrow -\infty}{\sim} (-q^2)^{-2}$

Pauli form factor F_2

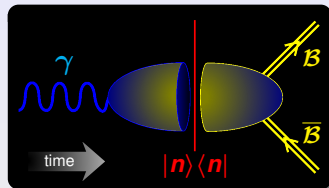
- Spin flip
- Two gluon propagators
- $F_2(q^2) \underset{q^2 \rightarrow -\infty}{\sim} (-q^2)^{-3}$

Sachs form factors G_E and G_M

- $G_{E,M}(q^2) \underset{q^2 \rightarrow -\infty}{\sim} (-q^2)^{-2}$
- Ratio: $\frac{G_E}{G_M} \underset{q^2 \rightarrow -\infty}{\sim} \text{constant}$

Baryon form factors

Time-like region ($q^2 > 0$)



- Crossing symmetry:

$$\langle \mathcal{B}(p') | j^\mu | \mathcal{B}(p) \rangle \rightarrow \langle \bar{\mathcal{B}}(p') \mathcal{B}(p) | j^\mu | 0 \rangle$$

- Form factors are complex functions of q^2

Optical theorem

$$\text{Im} \langle \bar{\mathcal{B}}(p') \mathcal{B}(p) | j^\mu | 0 \rangle \sim \sum_n \langle \bar{\mathcal{B}}(p') \mathcal{B}(p) | j^\mu | n \rangle \langle n | j^\mu | 0 \rangle \implies \begin{cases} \text{Im} F_{1,2} \neq 0 \\ \text{for } q^2 > 4M_\pi^2 \end{cases}$$

$|n\rangle$ are on-shell intermediate states: $2\pi, 3\pi, 4\pi, \dots$

Time-like asymptotic behavior

Phragmén Lindelöf theorem:

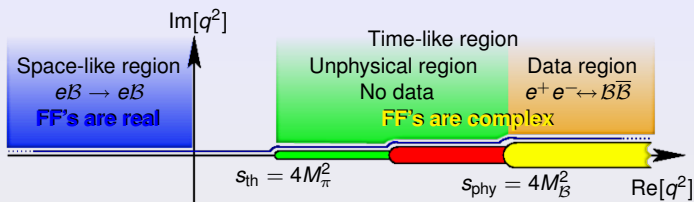
If $f(z) \rightarrow a$ as $|z| \rightarrow \infty$ along a straight line, and $f(z) \rightarrow b$ as $|z| \rightarrow \infty$ along another straight line, and $f(z)$ is regular and bounded in the angle between, then $a = b$ and $f(z) \rightarrow a$ uniformly in this angle.

$$\lim_{q^2 \rightarrow -\infty} G_{E,M}(q^2) = \lim_{q^2 \rightarrow +\infty} G_{E,M}(q^2)$$

space-like
time-like

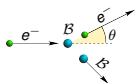
$$G_{E,M} \sim (q^2)^{-2} \quad \text{real}$$

Cross sections and analyticity



Time-like: had. helicity = $\begin{cases} 1 \Rightarrow |G_E| \\ 0 \Rightarrow |G_M| \end{cases}$

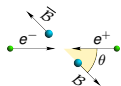
$G_E(4M_B^2) = G_M(4M_B^2)$



Elastic scattering

$$\frac{d\sigma}{d\Omega} = \frac{\alpha^2 E_e' \cos^2 \frac{\theta}{2}}{4E_e^3 \sin^4 \frac{\theta}{2}} \left[G_E^2 - \tau \left(1 + 2(1-\tau) \tan^2 \frac{\theta}{2} \right) G_M^2 \right] \frac{1}{1-\tau}$$

$\tau = \frac{q^2}{4M_B^2}$



Annihilation

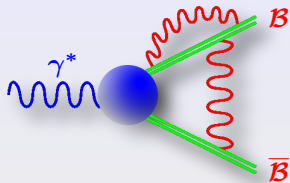
Coulomb correction

$$\frac{d\sigma}{d\Omega} = \frac{\alpha^2 \beta C}{4q^2} \left[(1 + \cos^2 \theta) |G_M|^2 + \frac{1}{\tau} \sin^2 \theta |G_E|^2 \right]$$

$\beta = \sqrt{1 - \frac{1}{\tau}}$



The Coulomb Factor



$p\bar{p}$ Coulomb interaction as FSI

[Sommerfeld, Sakharov, Schwinger, Fadin, Khoze]

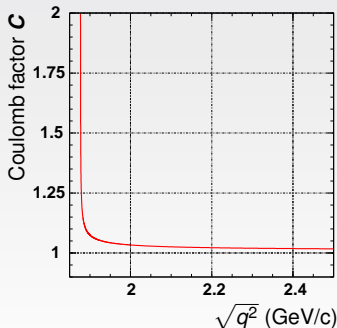
Distorted wave approximation

$$C = |\Psi_{\text{Coul}}(0)|^2$$

● S-wave:
$$C = \frac{\frac{\pi\alpha}{\beta}}{1 - \exp\left(-\frac{\pi\alpha}{\beta}\right)} \xrightarrow{\beta \rightarrow 0} \frac{\pi\alpha}{\beta}$$

● D-wave: $C = 1$

No Coulomb factor for boson pairs (P-wave)





Pointlike Baryons?

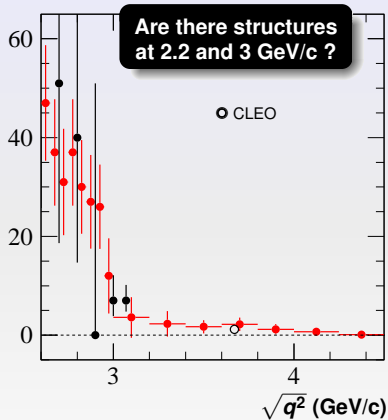
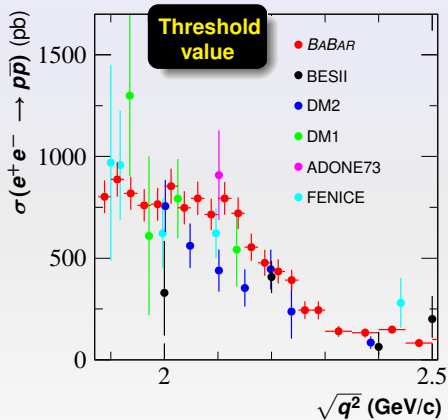
R. Baldini Ferroli, SP, A. Zallo
and A. Zichichi



October 1st, 2009

Time-like baryon form factors and dispersion relations

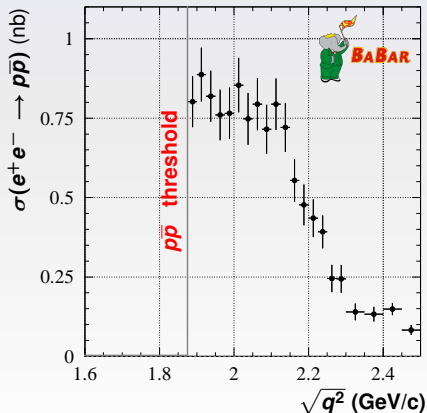
$e^+e^- \rightarrow p\bar{p}$: the world data sample



$$e^+e^- \rightarrow p\bar{p}\gamma \text{ (ISR)}$$

The incredible threshold value

$$\sigma(e^+e^- \rightarrow p\bar{p}) = \frac{4\pi\alpha^2\beta C}{3q^2} \left[|G_M^p|^2 + \frac{2M_p^2}{q^2} |G_E^p|^2 \right] \xrightarrow{\sqrt{q^2} \rightarrow 2M_p} \frac{\pi\alpha^2\beta C}{2M_p^2} |G^p|^2$$



At threshold
 $\sigma(e^+e^- \rightarrow p\bar{p}) = 0.83 \pm 0.05 \text{ nb}$

$e^+e^- \rightarrow p\bar{p}$ is the only endothermic process that shows this peculiarity

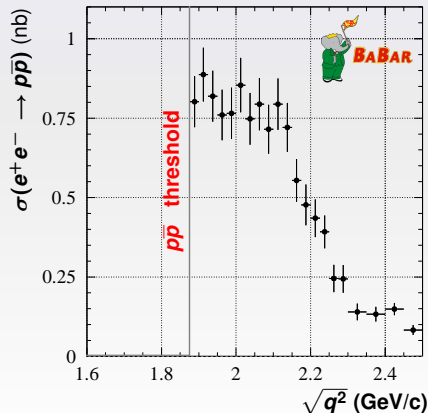
The factor C cancels the phase space

$$\beta C = \sqrt{1 - \frac{4M_p^2}{q^2}} C = \begin{cases} \text{finite at} \\ \text{threshold} \end{cases}$$

$e^+e^- \rightarrow p\bar{p}\gamma$ (ISR)

The incredible threshold value

$$\sigma(e^+e^- \rightarrow p\bar{p}) = \frac{4\pi\alpha^2\beta C}{3q^2} \left[|G_M^p|^2 + \frac{2M_p^2}{q^2} |G_E^p|^2 \right] \xrightarrow{\sqrt{q^2} \rightarrow 2M_p} \frac{\pi\alpha^2\beta C}{2M_p^2} |G^p|^2$$



At threshold
 $\sigma(e^+e^- \rightarrow p\bar{p}) = 0.83 \pm 0.05$ nb

$e^+e^- \rightarrow p\bar{p}$ is the only endothermic process that shows this peculiarity



The factor C cancels the phase space

$$\beta C = \sqrt{1 - \frac{4M_p^2}{q^2}} C = \begin{cases} \text{finite at} \\ \text{threshold} \end{cases}$$

Proton form factor at $q^2 = 4M_p^2$

$$\sigma(e^+e^- \rightarrow p\bar{p})(4M_p^2) = 0.83 \pm 0.05 \text{ nb}$$

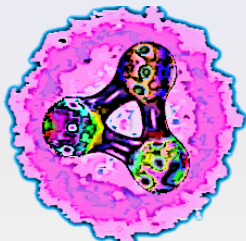
BABAR

$$\sigma(e^+e^- \rightarrow p\bar{p})(4M_p^2) = \frac{\pi^2 \alpha^3}{2M_p^2} \cancel{\beta} |G^p(4M_p^2)|^2 = 0.85 |G^p(4M_p^2)|^2 \text{ nb}$$

$$|G^p(4M_p^2)| \equiv 1$$

$$|G^p(4M_p^2)| = 0.99 \pm 0.04(\text{stat}) \pm 0.03(\text{syst})$$

$$|G^p(4M_p^2)| \equiv 1$$

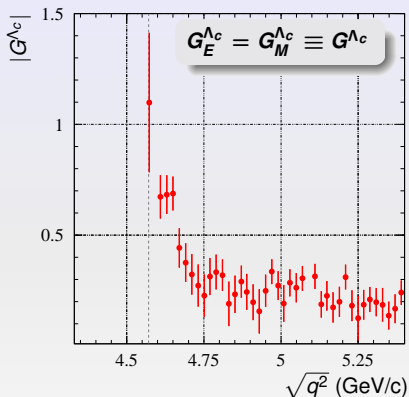
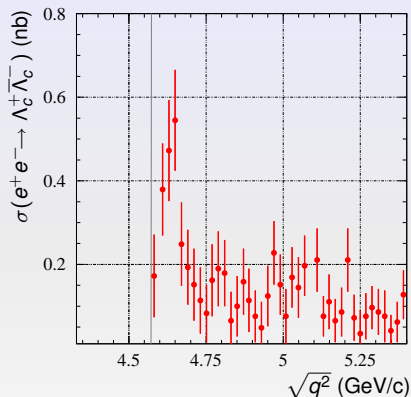


**At $q^2 = 4M_p^2$ protons behave
as pointlike fermions!**

A complex hand-drawn diagram on a white background, featuring a network of intersecting lines, circles, and arrows. The lines are mostly straight but some are curved, and they connect various points, some of which are marked with small circles or dots. The overall appearance is that of a technical sketch or a Feynman diagram, possibly representing particle interactions or form factors. The text is overlaid on this diagram.

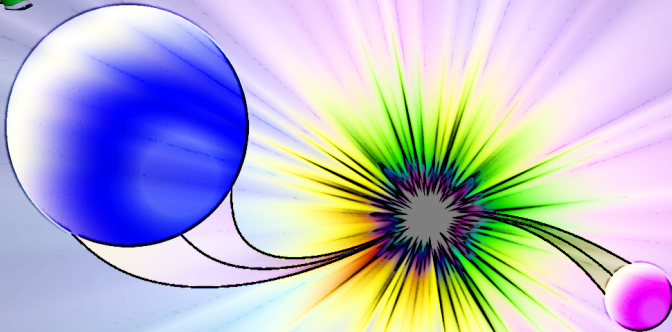
Other charged baryon FF's at threshold





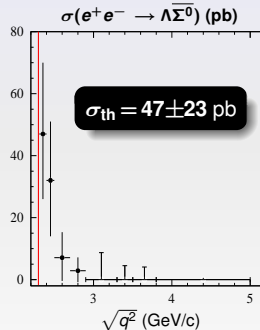
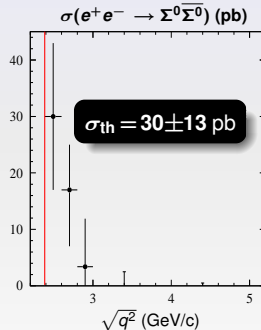
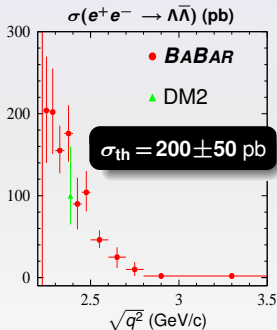
$$|G^{\Lambda_c}(4M_{\Lambda_c}^2)| = 1.1 \pm 0.3(\text{stat}) \pm 0.4(\text{syst})$$

The neutral baryons puzzle



$$\sigma(e^+e^- \rightarrow B^0\bar{B}^0) = \frac{4\pi\alpha^2\beta C_0}{3q^2} \left[|G_M^{B^0}|^2 + \frac{2M_{B^0}^2}{q^2} |G_E^{B^0}|^2 \right] \xrightarrow{\sqrt{q^2} \rightarrow 2M_{B^0}} \frac{\pi\alpha^2\beta}{2M_{B^0}^2} |G^{B^0}|^2 \rightarrow 0$$

No Coulomb correction at hadron level: $C_0 = 1$



Like a remnant of
Coulomb interactions
at quark level?

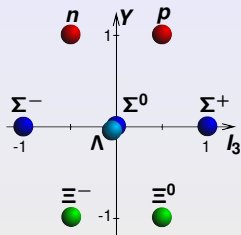


$C_0 \propto \beta^{-1}$
as $\sqrt{q^2} \rightarrow 2M_{B^0}$



For any neutral baryon

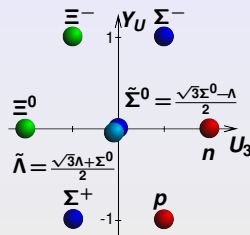
$$\sqrt{\sigma_{B^0\bar{B}^0}} \propto \frac{|G^{B^0}|}{M_{B^0}}$$



$$(Y, I_3) \rightarrow (Y_U, U_3)$$

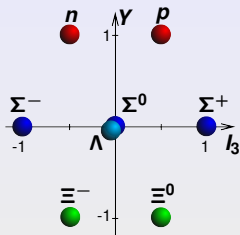
$$U_3 = -\frac{1}{2} I_3 + \frac{3}{4} Y$$

$$Y_U = -Q$$

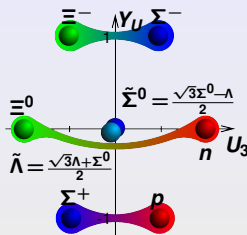


U-spin relation: $G^{\Sigma^0} - G^{\Lambda} + \frac{2}{\sqrt{3}} G^{\Lambda\Sigma^0} = 0$

$$M_{\Sigma^0} \sqrt{\sigma_{\Sigma^0 \Sigma^0}} - M_{\Lambda} \sqrt{\sigma_{\Lambda \bar{\Lambda}}} + \frac{2}{\sqrt{3}} M_{\Lambda \Sigma^0} \sqrt{\sigma_{\Lambda \Sigma^0}} = (-0.06 \pm 6.0) \times 10^{-4}$$



$$\begin{aligned} (Y, I_3) &\rightarrow (Y_U, U_3) \\ U_3 &= -\frac{1}{2} I_3 + \frac{3}{4} Y \\ Y_U &= -Q \end{aligned}$$

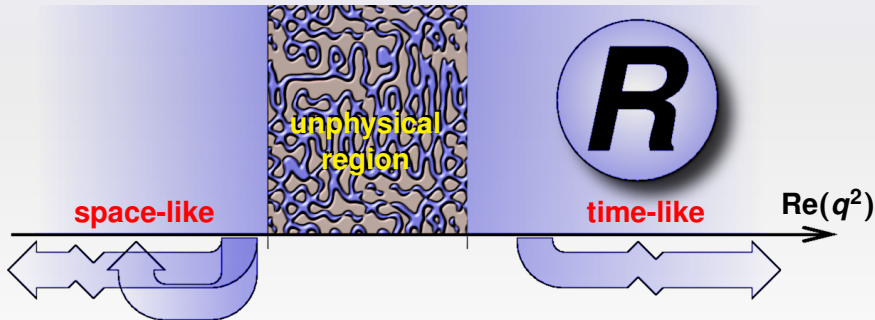


U-spin relation: $G^{\Sigma^0} - G^{\Lambda} + \frac{2}{\sqrt{3}} G^{\Lambda\Sigma^0} = 0$

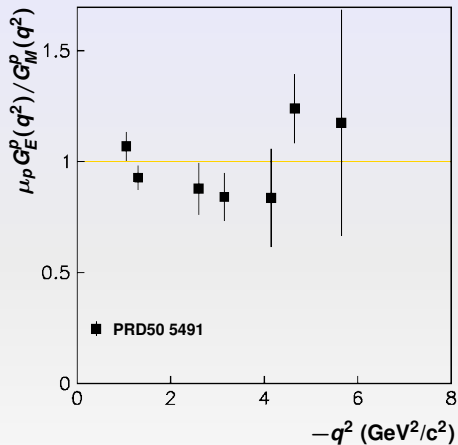
$$M_{\Sigma^0} \sqrt{\sigma_{\Sigma^0 \Sigma^0}} - M_{\Lambda} \sqrt{\sigma_{\Lambda \Lambda}} + \frac{2}{\sqrt{3}} M_{\Lambda \Sigma^0} \sqrt{\sigma_{\Lambda \Sigma^0}} = (-0.06 \pm 6.0) \times 10^{-4}$$

Dispersive analysis of the ratio $R = \mu_p \frac{G_E^p}{G_M^p}$

Eur. Phys. J. A32, 421
R. Baldini, S. Pacetti and A. Zallo



Space-like G_E^p/G_M^p measurements



$$G_E^p = F_1^p + \frac{q^2}{4M_p^2} F_2^p$$

$$G_M^p = F_1^p + F_2^p$$

Space-like

$$F_1 / \frac{q^2}{4M_p^2} F_2 \text{ cancellation}$$

$$\frac{G_E^p(q^2)}{G_M^p(q^2)} < 1$$

Time-like

$$F_1 / \frac{q^2}{4M_p^2} F_2 \text{ enhancement}$$

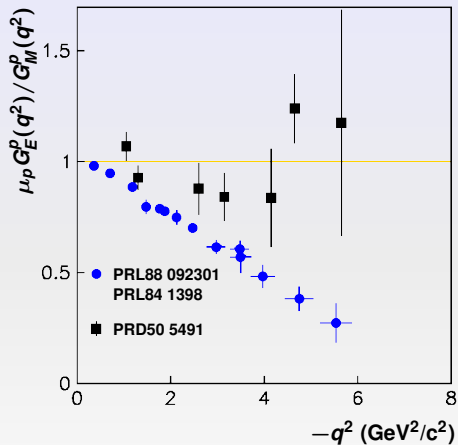
$$\left| \frac{G_E^p(q^2)}{G_M^p(q^2)} \right| > 1$$

Radiative corrections of
polarization technique



Radiative corrections in
Rosenbluth method

Space-like G_E^p/G_M^p measurements



$$G_E^p = F_1^p + \frac{q^2}{4M_p^2} F_2^p$$

$$G_M^p = F_1^p + F_2^p$$

Space-like

$F_1 / \frac{q^2}{4M_p^2} F_2$ cancellation

$$\frac{G_E^p(q^2)}{G_M^p(q^2)} < 1$$

Time-like

$F_1 / \frac{q^2}{4M_p^2} F_2$ enhancement

$$\left| \frac{G_E^p(q^2)}{G_M^p(q^2)} \right| > 1$$

Radiative corrections of
polarization technique

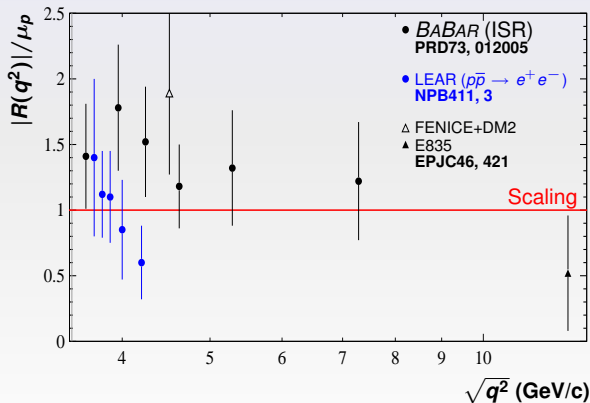


Radiative corrections in
Rosenbluth method

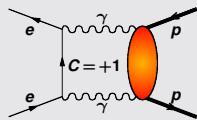
Time-like $|G_E^p/G_M^p|$ measurements

$$\frac{d\sigma}{d\cos\theta} = \frac{\pi\alpha^2\beta C}{2q^2} |G_M^p|^2 \left[(1 + \cos^2\theta) + \frac{4M_p^2}{q^2\mu_p^2} \sin^2\theta |R|^2 \right]$$

$$R(q^2) = \mu_p \frac{G_E^p(q^2)}{G_M^p(q^2)}$$



$\gamma\gamma$ exchange



$\gamma\gamma$ exchange interferes with the Born term



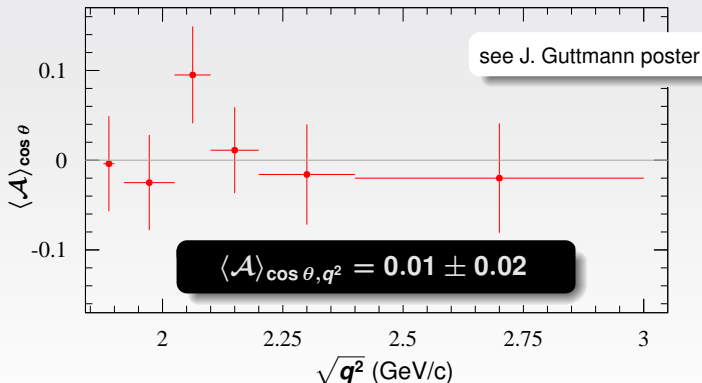
Asymmetry in angular distributions

[PLB659, 197]

$\gamma\gamma$ exchange from $e^+e^- \rightarrow p\bar{p}\gamma$ *BABAR* data

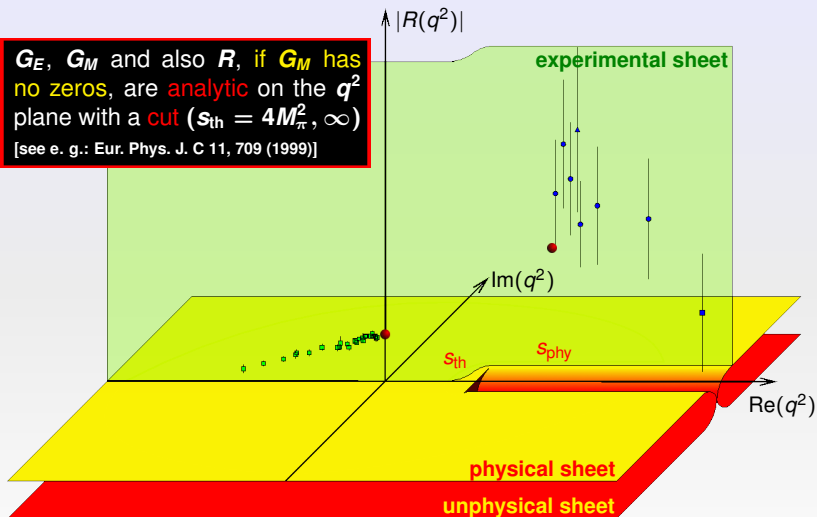
E. Tomasi-Gustafsson,
E. A. Kuraev, S. Bakmaev, SP
PLB659, 197

$$\mathcal{A}(\cos\theta, q^2) = \frac{\frac{d\sigma}{d\Omega}(\cos\theta, q^2) - \frac{d\sigma}{d\Omega}(-\cos\theta, q^2)}{\frac{d\sigma}{d\Omega}(\cos\theta, q^2) + \frac{d\sigma}{d\Omega}(-\cos\theta, q^2)}$$

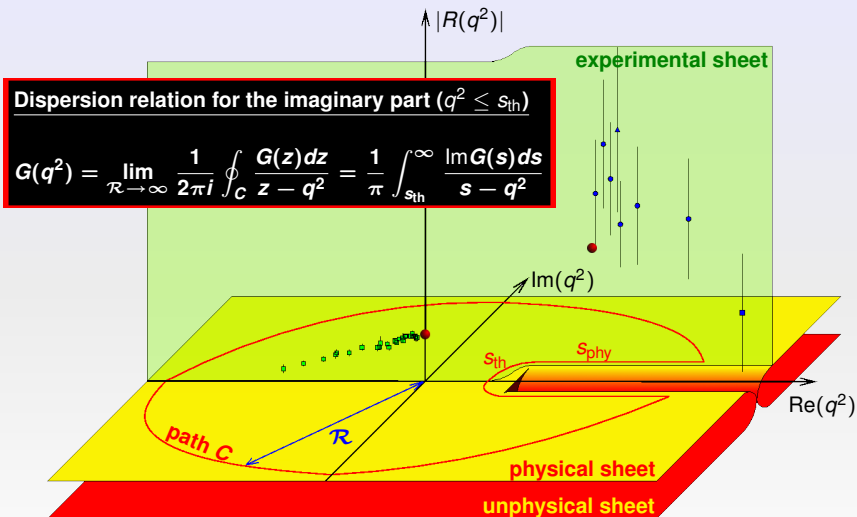


$R(q^2)$ in the complex plane

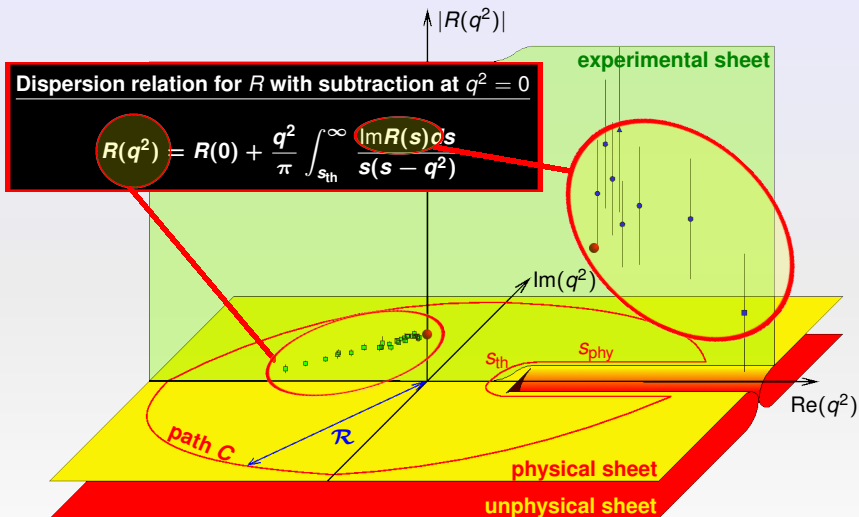
G_E , G_M and also R , if G_M has no zeros, are analytic on the q^2 plane with a cut ($s_{th} = 4M_\pi^2, \infty$) [see e. g.: Eur. Phys. J. C 11, 709 (1999)]



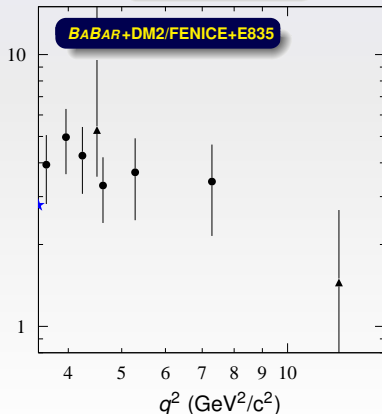
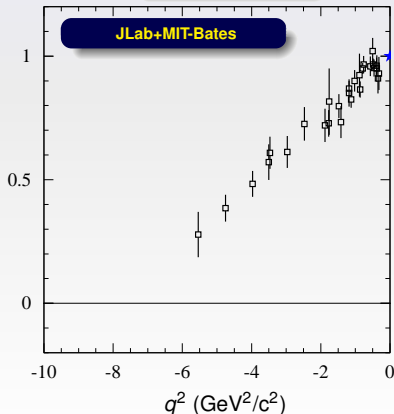
$R(q^2)$ in the complex plane



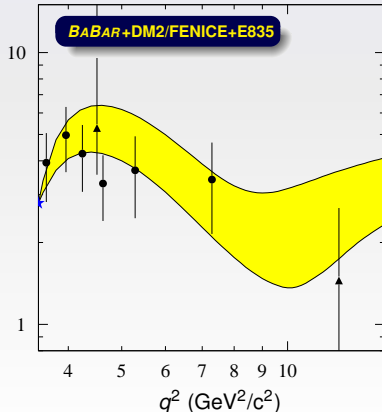
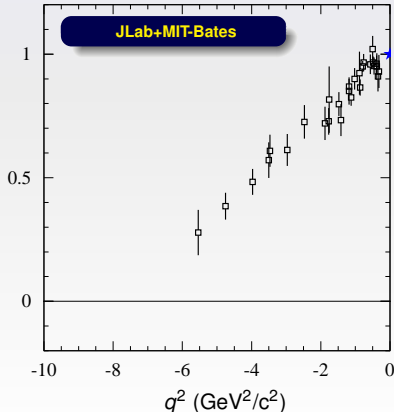
$R(q^2)$ in the complex plane



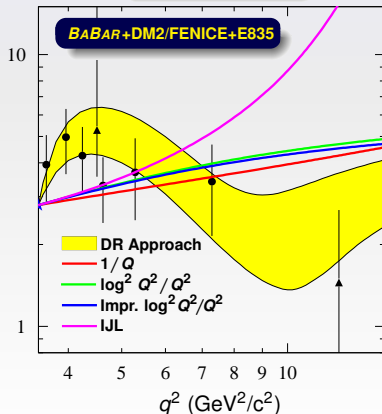
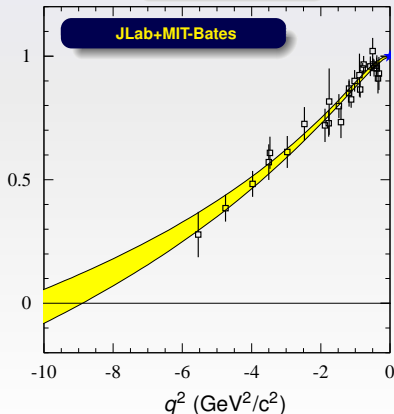
$$R(q^2) = R(0) + \frac{q^2}{\pi} \int_{4M_\pi^2}^{\infty} \frac{\text{Im}R(s)}{s(s - q^2)} ds$$

 $\text{Re}q^2$ $R(q^2)$ space-like $|R(q^2)|$ time-like

$$R(q^2) = R(0) + \frac{q^2}{\pi} \int_{4M_\pi^2}^{\infty} \frac{\text{Im}R(s)}{s(s - q^2)} ds$$

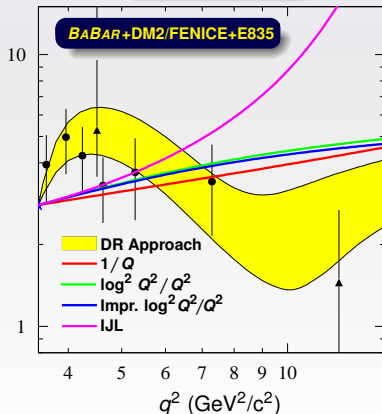
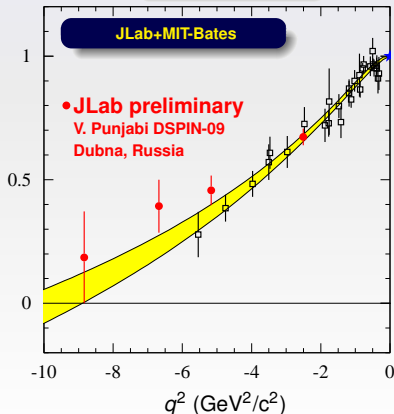
 $\text{Re}q^2$ $R(q^2)$ space-like $|R(q^2)|$ time-like

$$R(q^2) = R(0) + \frac{q^2}{\pi} \int_{4M_\pi^2}^{\infty} \frac{\text{Im}R(s)}{s(s - q^2)} ds$$

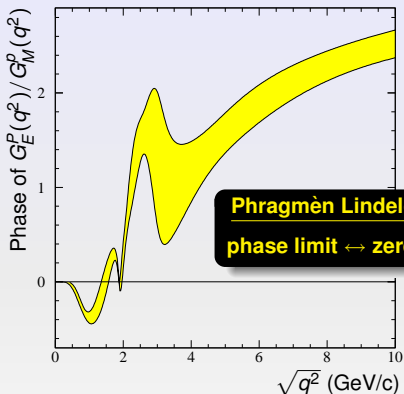
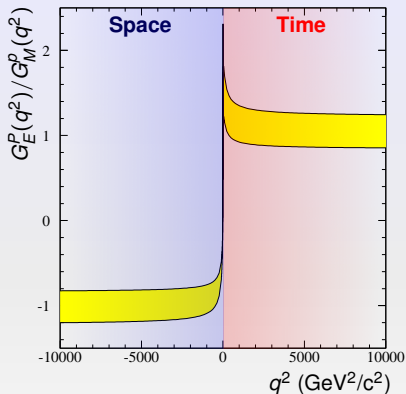
 $\text{Re}q^2$ $R(q^2)$ space-like $|R(q^2)|$ time-like

$$R(q^2) = R(0) + \frac{q^2}{\pi} \int_{4M_\pi^2}^{\infty} \frac{\text{Im}R(s)}{s(s - q^2)} ds$$


 Re q^2
 $R(q^2)$ space-like

 $|R(q^2)|$ time-like


Asymptotic $G_E^p(q^2)/G_M^p(q^2)$ and phase



pQCD prediction

$$\frac{G_E^p(q^2)}{G_M^p(q^2)} \xrightarrow{|q^2| \rightarrow \infty} -1$$

Phase from DR

$$\phi(q^2) = -\frac{\sqrt{q^2 - s_0}}{\pi} \text{Pr} \int_{s_0}^{\infty} \frac{\ln |R(s)| ds}{\sqrt{s - s_0}(s - q^2)}$$

Highlights

- Coulomb correction for $B\bar{B}$
 - Charged baryons **as pointlike fermions**
 - Puzzling cross sections at threshold for neutral baryons
- Time + space-like data for G_E^p/G_M^p predict:
 - a **space-like zero**, also from time-like phase
 - the space-like limit $G_E^p/G_M^p \rightarrow -1$

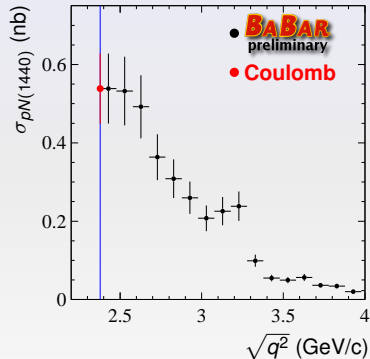
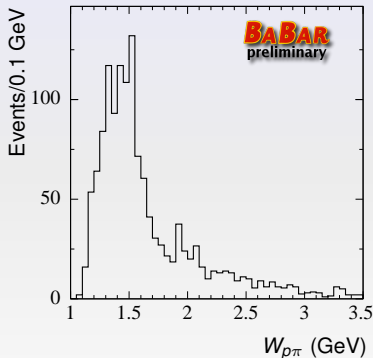
Expectations

- Theoretical space-like **and time-like** interpretations
- New **polarized** and unpolarized, space and time data: BESIII, VEPP2000, Belle2, Panda (M. Sudot), SuperB (?)

BACK-UP SLIDES



$$\sigma_{\text{Coulomb}} = \frac{16\pi^2\alpha^3 M_p^{3/2} M_{N(1440)}^{3/2}}{(M_p + M_{N(1440)})^5} |G^{pN(1440)}|^2 = |G^{pN(1440)}|^2 \times 0.49 \text{ nb}$$



$$|G^{pN(1440)}| = 1.04 \pm 0.09$$

Advantages

- DR's are based on unitarity and analyticity \Rightarrow **model-independent approach**
- DR's relate data from different processes in different energy regions

$$\left[\begin{array}{c} \text{space-like} \\ \text{form factor} \\ eB \rightarrow e\bar{B} \end{array} \right] = \int \left[\begin{array}{c} \text{Im}(\text{form factor}) \text{ or } \text{ln}|\text{form factor}| \\ \text{over the time-like cut } (s_{\text{th}}, \infty) \\ e^+ e^- \rightarrow B\bar{B} + \text{theory} \end{array} \right]$$

- Normalizations and theoretical constraints can be directly implemented
- Form factors can be computed in the whole q^2 -complex plane

Drawbacks

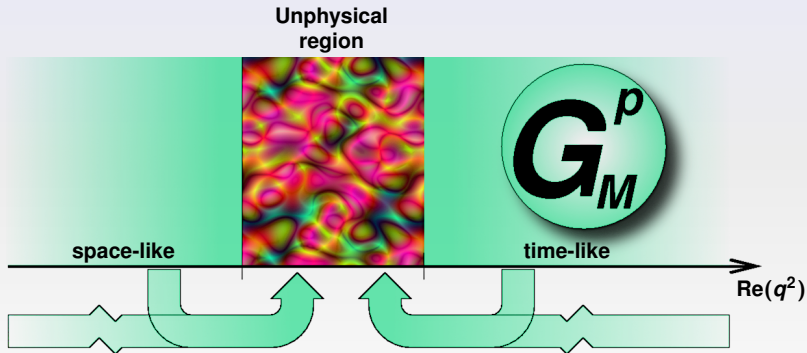
- Very long range integration

Even though pQCD provides power rules nobody knows at which energy the form factors start to follow these behaviors

Subtracted dispersion relations help in making the approach as less as possible dependent on the asymptotic behavior

- No data in the unphysical region

Proton magnetic form factor with unphysical-contribution suppression



Dispersion relations and sum rules

Geshkenbein, Ioffe, Shifman Yad. Fiz. 20, 128 (1974)

- DR's connect space and time values of a form factor $G(q^2)$

$$G(q^2) = \frac{1}{\pi} \int_{s_{\text{th}}}^{\infty} \frac{\text{Im}G(s) ds}{s - q^2}$$



Drawbacks

- The imaginary part is not experimentally accessible
- There are no data in the unphysical region $[s_{\text{th}}, s_{\text{phy}}]$
- We need to know the asymptotic behavior

- They applied the DR for the imaginary part to the function

$$\phi(z) = f(z) \frac{\ln G(z)}{z\sqrt{s_{\text{th}} - z}} \quad \text{with} \quad \int_0^{s_{\text{phy}}} f^2(z) dz \ll 1$$

Advantages

- The DR integral contains the modulus $|G(s)|$
- The unphysical region contribution is suppressed

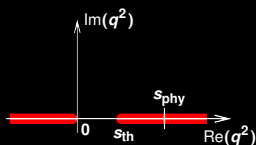
Drawback

- Zeros of $G(z)$ are poles for $\phi(z)$

Attenuation of the unphysical region

Strategy

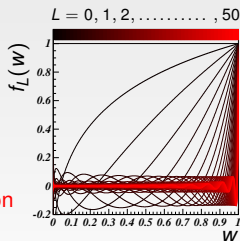
- Use the function $\phi(z) = f(z) \frac{\ln G(z)}{z\sqrt{s_{\text{th}} - z}}$
- $f(z)$, is analytic with the cut $(-\infty, 0)$
- $f(z) = f_L(w) = \sum_{l=0}^L \frac{2l+1}{(L+1)^2} P_l(1-2w)$, $w = \frac{\sqrt{s_{\text{phy}}} - \sqrt{z}}{\sqrt{s_{\text{phy}}} + \sqrt{z}}$



- This function, with $f_L(0)=1$, minimizes:

$$\int_0^1 f_L^2(w) dw$$

and suppresses the contribution in the unphysical region



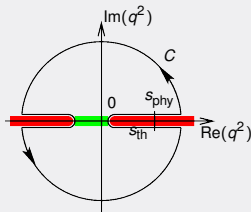
Attenuated DR and sum rule

New DR with variable suppressed region $[0, s_{\text{phy}}]$

$[G(q^2)$ has no zeros]

$$\oint_C \phi(z) dz = 0$$

$$\underbrace{-\int_{-\infty}^0 \frac{\text{Im}[f(t)] \ln G(t)}{t\sqrt{s_{\text{th}} - t}} dt}_{\text{Space-like}} \Downarrow \underbrace{\int_{s_{\text{th}}}^{\infty} \frac{f(s) \ln |G(s)|}{s\sqrt{s - s_{\text{th}}}} ds}_{\text{Time-like}}$$



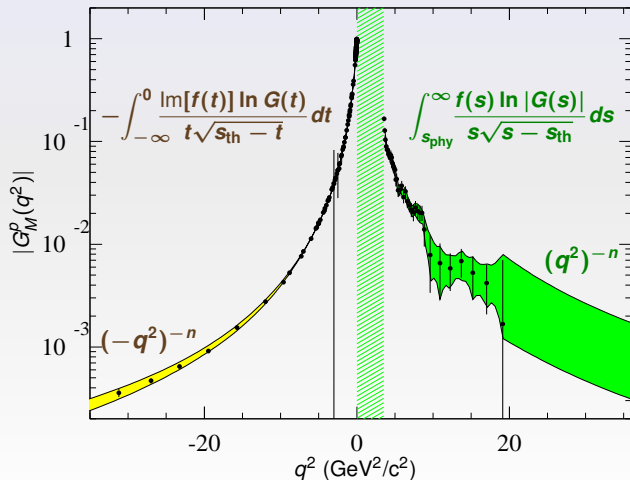
Convergence relation to test asymptotic power behaviour of G_M^p

$$\underbrace{-\int_{-\infty}^0 \frac{\text{Im}[f(t)] \ln G(t)}{t\sqrt{s_{\text{th}} - t}} dt}_{\text{Space-like data} + (-t)^{-n}} = \int_{s_{\text{th}}}^{\infty} \frac{f(s) \ln |G(s)|}{s\sqrt{s - s_{\text{th}}}} ds \approx \underbrace{\int_{s_{\text{phy}}}^{\infty} \frac{f(s) \ln |G(s)|}{s\sqrt{s - s_{\text{th}}}} ds}_{\text{Time-like data} + s^{-n}}$$

n is the free parameter

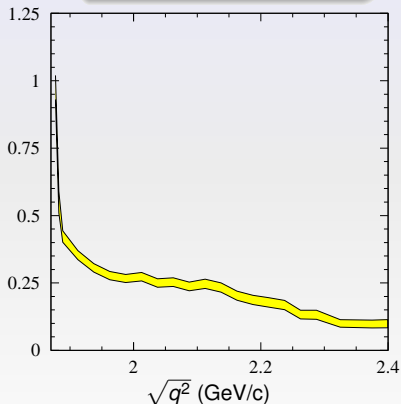
Sum rule: result

$$G_M^p(q^2) \underset{|q^2| \rightarrow \infty}{\propto} (q^2)^{-(2.27 \pm 0.36)}$$

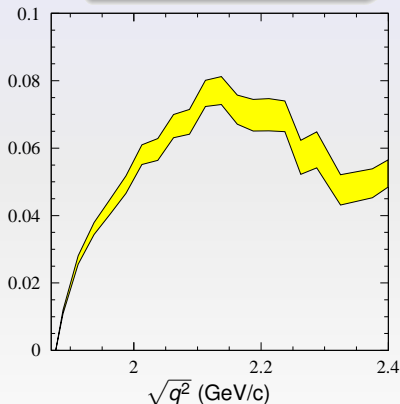


Phases from DR: $|B_S^p(q^2)|$ and $|B_D^p(q^2)|$

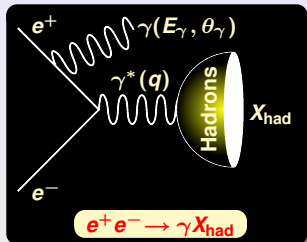
$$|B_S^p(q^2)| = \frac{|2\sqrt{\tau}G_M^p + G_E^p|}{3}$$



$$|B_D^p(q^2)| = \frac{|\sqrt{\tau}G_M^p - G_E^p|}{3}$$



Initial State Radiation



$$\frac{d^2\sigma}{dE_\gamma d\theta_\gamma} = W(E_\gamma, \theta_\gamma) \cdot \sigma_{e^+e^- \rightarrow X_{had}}(s)$$

- $s = q^2, q \dots X_{had}$ momentum
- $E_\gamma \dots \dots \dots$ CM γ energy
- $\theta_\gamma \dots$ CM γ scattering angle
- $E_{CM} \dots \dots$ CM e^+e^- energy

Radiator function in Born approximation

$$W(E_\gamma, \theta_\gamma) = \frac{\alpha}{\pi x} \left(\frac{2 - 2x + x^2}{\sin^2 \theta_\gamma} \right), \quad x = \frac{E_\gamma}{2E_{CM}}$$

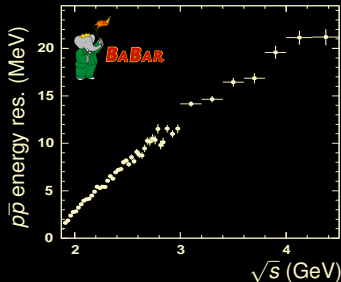
$$\theta_\gamma \gg \frac{m_e}{E_{CM}}$$

For $20^\circ < \theta_\gamma < 160^\circ$ ISR angular acceptance $\sim 17\%$

ISR versus CM scan

Advantages

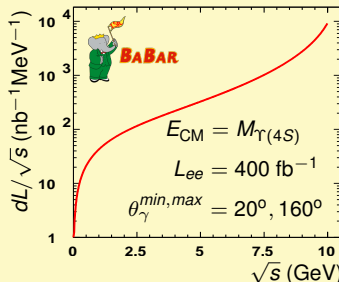
- All energies (q^2) at the same time
↓
Better control on systematics
(e.g. greatly reduced point to point)
- Detected ISR \Rightarrow full X_{had} ang. coverage
- CM boost \Rightarrow $\left\{ \begin{array}{l} \text{at threshold } \epsilon \neq 0 \\ \text{energy res. } \sim 1 \text{ MeV} \end{array} \right.$



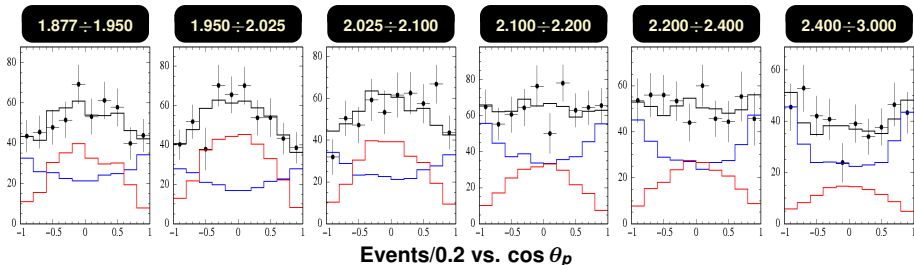
Drawbacks

- ISR $\mathcal{L} \propto$ energy bin width
- More background: non-ISR events

$$\frac{dL}{d\sqrt{s}} = \frac{2\sqrt{s}}{E_{\text{CM}}^2} L_{ee} \int_{\cos \theta_{\gamma}^{\min}}^{\cos \theta_{\gamma}^{\max}} d \cos \theta_{\gamma} W(E_{\gamma}, \theta_{\gamma})$$



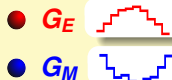
$\cos \theta_p$ distributions from threshold up to 3 GeV [intervals in $E_{CM} \equiv q$ (GeV)]



$$\frac{d\sigma}{d\cos\theta_p} = A \left[H_E(\cos\theta_p, q^2) \left| \frac{G_E^p(q^2)}{G_M^p(q^2)} \right|^2 + H_M(\cos\theta_p, q^2) \right]$$

H_E and H_M from MC

Histograms show contributions from



At low q

$$\sin^2 \theta_p > 1 + \cos^2 \theta_p \Rightarrow$$

First observation!

$$|G_E^p| > |G_M^p|$$

At higher q , $|G_E^p| \rightarrow |G_M^p|$

Parameterization and constraints

The imaginary part of R is parameterized by two series of orthogonal polynomials $T_j(x)$

$$\text{Im}R(q^2) \equiv I(q^2) = \begin{cases} \sum_i C_i T_i(x) & x = \frac{2q^2 - s_{\text{phy}} - s_{\text{th}}}{s_{\text{phy}} - s_{\text{th}}} \quad s_{\text{th}} \leq q^2 \leq s_{\text{phy}} \\ \sum_j D_j T_j(x') & x' = \frac{2s_{\text{phy}}}{q^2} - 1 \quad q^2 > s_{\text{phy}} \end{cases}$$

$s_{\text{th}} = 4M_\pi^2$
 $s_{\text{phy}} = 4M_N^2$

Theoretical conditions on $\text{Im}R(q^2)$

- $R(4M_\pi^2)$ is real $\implies I(4M_\pi^2) = 0$
- $R(4M_N^2)$ is real $\implies I(4M_N^2) = 0$
- $R(\infty)$ is real $\implies I(\infty) = 0$

Theoretical conditions on $R(q^2)$

- Continuity at $q^2 = 4M_\pi^2$
- $R(4M_N^2)$ is real and $\text{Re}R(4M_N^2) = \mu_p$

Experimental conditions on $R(q^2)$ and $|R(q^2)|$

- Space-like region ($q^2 < 0$) data for R from TJNAF and MIT-Bates
- Time-like region ($q^2 \geq 4M_N^2$) data for $|R|$ from FENICE+DM2, BABAR, E835 and LEAR

- Real asymptotic values for R

$$R_{BABAR}(\infty) = -(1.0 \pm 0.2)\mu_p$$

BABAR is in agreement with the scaling law $|G_E(q^2)| \simeq |G_M(q^2)|$ as $q^2 \rightarrow \infty$

- Asymptotic behaviour of F_2/F_1

$$\lim_{q^2 \rightarrow \infty} \frac{q^2}{4M_N^2} \left| \frac{F_2}{F_1} \right| = \left| \frac{R(\infty)}{\mu_p} - 1 \right| = 2.0 \pm 0.2 \text{ (BABAR)}$$

$$\left| \frac{F_2}{F_1} \right| \underset{q^2 \rightarrow \infty}{\propto} \frac{1}{q^2}$$

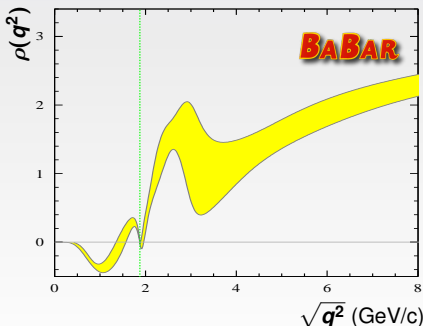
- Space-like zero

$$t_0^{BABAR} = (-10 \pm 1) \text{ GeV}^2/c^2$$

- Phragmén-Lindelöf theorem

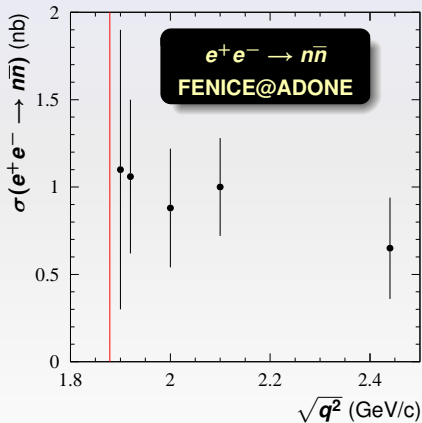
$$\rho(q^2) \xrightarrow{q^2 \rightarrow \infty} \pi \text{ with}$$

$$R(q^2) = |R(q^2)| e^{i\rho(q^2)}$$



U-spin prediction for neutrons at threshold

$$\sigma(e^+e^- \rightarrow n\bar{n}) = (3\sqrt{\sigma_{\Lambda\bar{\Lambda}}}M_\Lambda - \sqrt{\sigma_{\Sigma^0\bar{\Sigma}^0}}M_\Sigma)^2 \frac{1}{4M_n^2} = 0.5 \pm 0.2 \text{ nb}$$

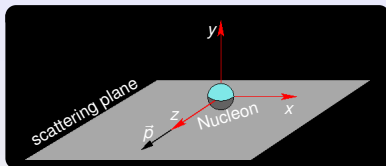


Polarization formulae in the time-like region

The ratio $R(q^2)$ is complex for $q^2 \geq s_{th}$

$$R(q^2) = \mu_p \frac{G_E^p(q^2)}{G_M^p(q^2)} = |R(q^2)| e^{i\rho(q^2)}$$

The polarization depends on the phase ρ



$$\mathcal{P}_y = - \frac{\sin(2\theta) |R| \sin(\rho)}{D \sqrt{\tau}}$$

Does not depend on P_e

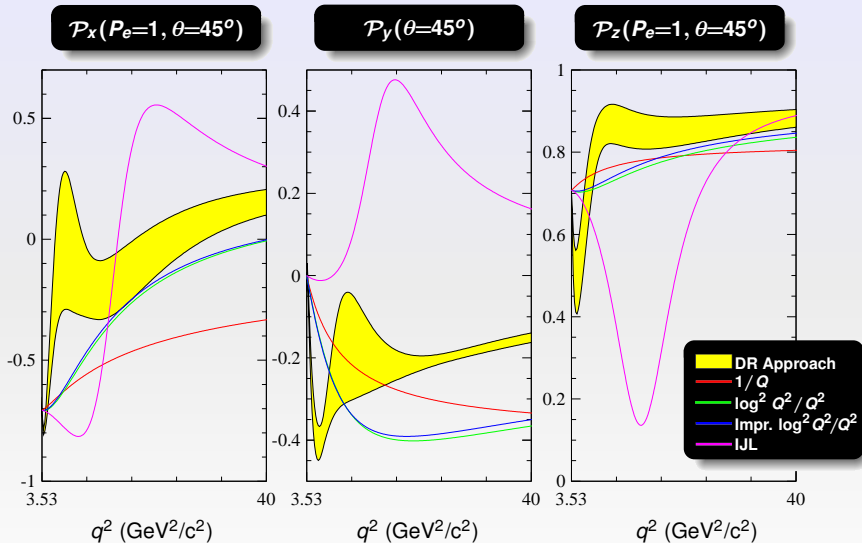
$$\mathcal{P}_x = - P_e \frac{2 \sin(2\theta) |R| \cos(\rho)}{D \sqrt{\tau}}$$

$$\mathcal{P}_z = P_e \frac{2 \cos(\theta)}{D}$$

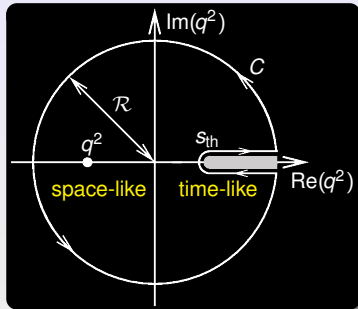
Does not depend on ρ

$$D = \frac{1 + \cos^2 \theta + \frac{1}{\tau} |R|^2 \sin^2 \theta}{\mu_p} \quad \tau = \frac{q^2}{4M_N^2} \quad P_e = \text{electron polarization}$$

Single Polarization



Dispersion relations



- The form factors are **analytic** on the q^2 -plane with a **multiple cut** ($s_{\text{th}} = 4M_\pi^2, \infty$)

- Dispersion relation for the imaginary part** ($q^2 < 0$)

$$G(q^2) = \lim_{R \rightarrow \infty} \frac{1}{2\pi i} \oint_C \frac{G(z) dz}{z - q^2} = \frac{1}{\pi} \int_{s_{\text{th}}}^{\infty} \frac{\text{Im} G(s) ds}{s - q^2}$$

- Dispersion relation for the logarithm** ($q^2 < 0$)

B.V. Geshkenbein, Yad. Fiz. 9 (1969) 1232.

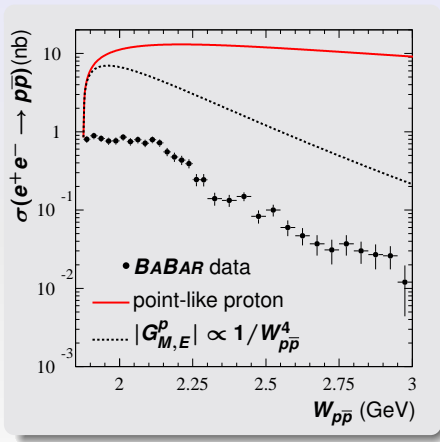
$$\ln G(q^2) = \frac{\sqrt{s_{\text{th}} - q^2}}{\pi} \int_{s_{\text{th}}}^{\infty} \frac{\ln |G(s)| ds}{(s - q^2) \sqrt{s - s_{\text{th}}}}$$

Experimental inputs

- Space-like data on the real values of FF's from: $e^- \mathcal{B} \rightarrow e^- \mathcal{B}$ and $e^- \uparrow \mathcal{B} \rightarrow e^- \mathcal{B} \uparrow$, with polarization
- Time-like data on moduli of FF's from: $e^+ e^- \rightarrow \mathcal{B} \overline{\mathcal{B}}$
- Time-like data on G_E - G_M relative phase from: $e^+ e^- \rightarrow \mathcal{B} \uparrow \overline{\mathcal{B}}$ (pol.)

Theoretical ingredients

- Analyticity \Rightarrow dispersion relations
- Normalization and threshold values
- Asymptotic behavior \Rightarrow super-convergence relations



Simple models for FF's

- Point-like proton (red curve)

$$G_E^p = G_M^p \equiv 1$$

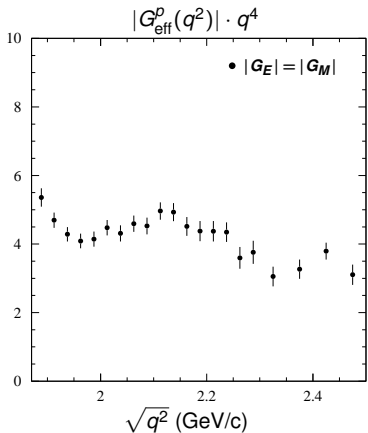
- Counting rule (dashed curve)

$$|G_{M,E}^p| \propto 1/W_{p\bar{p}}^4$$

$$\downarrow$$

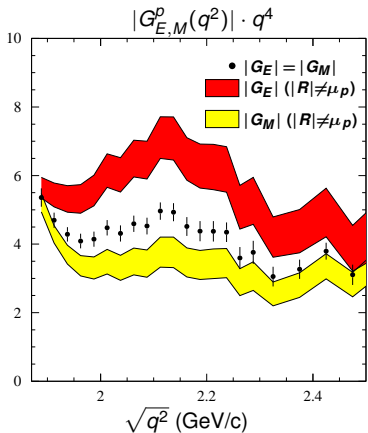
$$\sigma(e^+e^- \rightarrow p\bar{p}) \propto 1/W_{p\bar{p}}^{10}$$

Additional factors related to β and non-trivially structured electric and magnetic FF's must be included to reproduce the flat behavior of the data



$$|G_{\text{eff}}^p(q^2)|^2 = \frac{\sigma_{p\bar{p}}(q^2)}{\frac{4\pi\alpha^2\beta C}{3s}} \left(1 + \frac{1}{2\tau}\right)^{-1}$$

- Usually what is extracted from the cross section $\sigma(e^+e^- \rightarrow p\bar{p})$ is the effective time-like form factor $|G_{\text{eff}}^p|$ obtained assuming $|G_E^p| = |G_M^p|$ i.e. $|R| = \mu_p$
- Using our parametrization for R and the *BABAR* data on $\sigma(e^+e^- \leftrightarrow p\bar{p})$, $|G_E^p|$ and $|G_M^p|$ may be disentangled



$$|G_M(q^2)|^2 = \frac{\sigma_{p\bar{p}}(q^2)}{\frac{4\pi\alpha^2\beta C}{3s}} \left(1 + \frac{|R(q^2)|}{2\mu_p\tau}\right)^{-1}$$

- Usually what is extracted from the cross section $\sigma(e^+e^- \rightarrow p\bar{p})$ is the effective time-like form factor $|G_{\text{eff}}^p|$ obtained assuming $|G_E^p| = |G_M^p|$ i.e. $|R| = \mu_p$
- Using our parametrization for R and the *BABAR* data on $\sigma(e^+e^- \leftrightarrow p\bar{p})$, $|G_E^p|$ and $|G_M^p|$ may be disentangled